

Progress in CTEQ-TEA global analysis

Pavel Nadolsky

On behalf of all collaboration members

ANL/Shanghai University: J. Gao

University of Manchester: M. Guzzi

Michigan State University: J. Huston, J. Pumplin,
D. Stump, C. Schmidt, J. Winter, C.-P. Yuan

Southern Methodist University: T.-J. Hou,
P. Nadolsky, B. T. Wang, K. P. Xie

Xinjiang University: S. Dulat



CT14 family of NNLO parton distribution functions

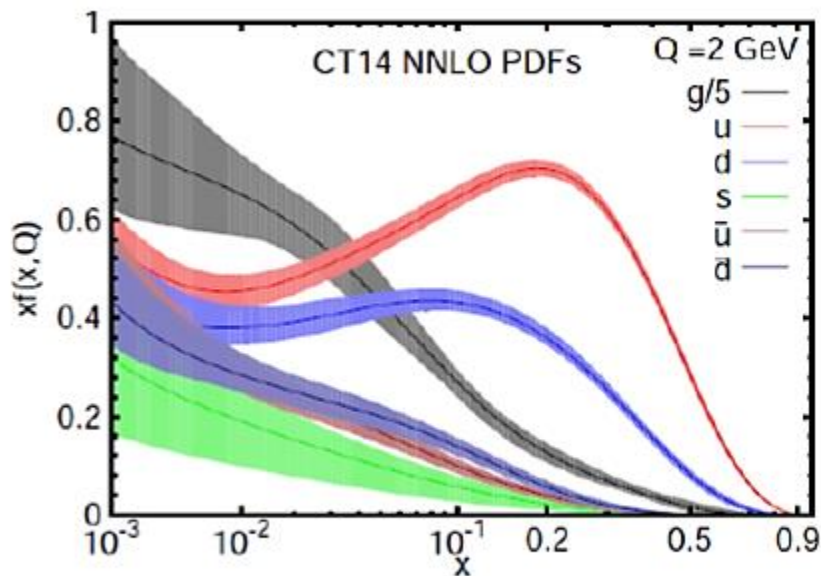
1. **CT14** general-purpose NNLO PDFs with LHC data and latest Tevatron data (*arXiv:1506.07443*)
2. **CT14 QED PDFs with photon PDFs** (*arXiv:1509.02905*)
3. **CT14 HERA2**: updated CT14 PDFs with HERA1+2 data (*submitted to arXiv, can be used in specialized studies*)
1. **CT14 MC1 and MC2**: Monte Carlo replicas with asymmetric uncertainties and positivity (*T.-J. Hou et al., arXiv:1607.06066*)
 - Public program **mcgen** to generate such replicas on **metapdf.hepforge.org/mcgen**
5. **CT14 IC (HERA2)**: Updated CT14 PDFs with intrinsic charm and legacy HERA data (*T.-J. Hou et al., arXiv:1610.xxxxx*)

CT14 general-purpose PDFs...

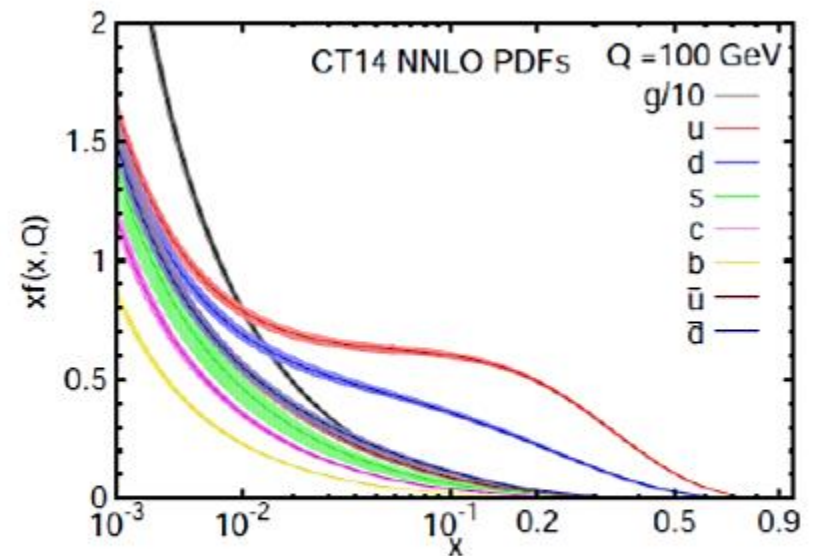
... include LHC Run 1 data and new Tevatron D0 Run 2 data on W-electron charge asymmetry

... use a more flexible parametrization for PDFs, compared to CT10

... are available at NNLO, NLO and LO, for $\alpha_s(M_Z) = 0.118 \pm 0.002$ at 90% c.l.; for 3, 4, 5, 6 active flavors



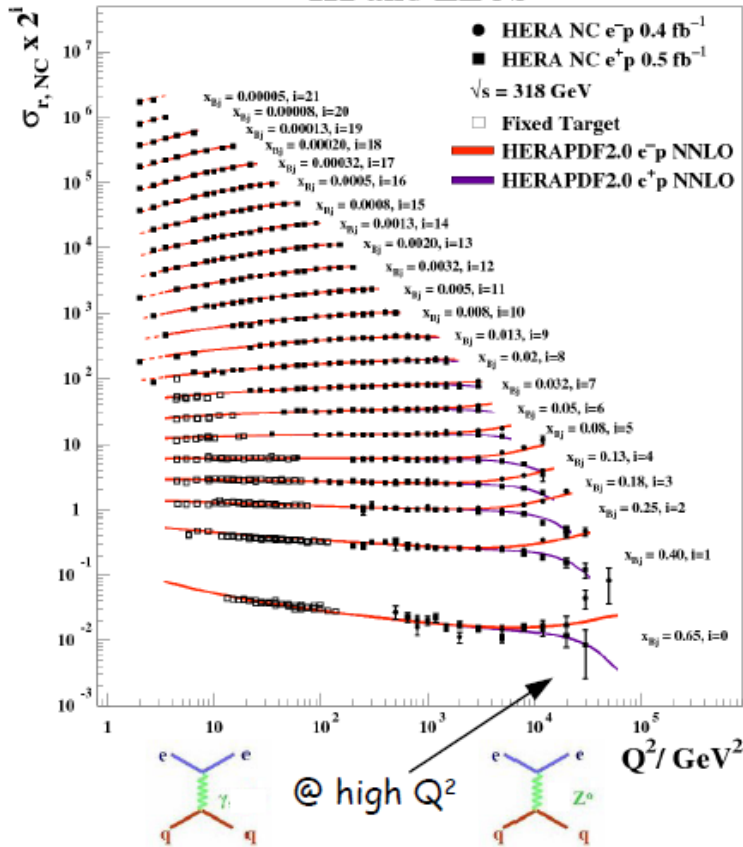
$Q = 2 \text{ GeV}$



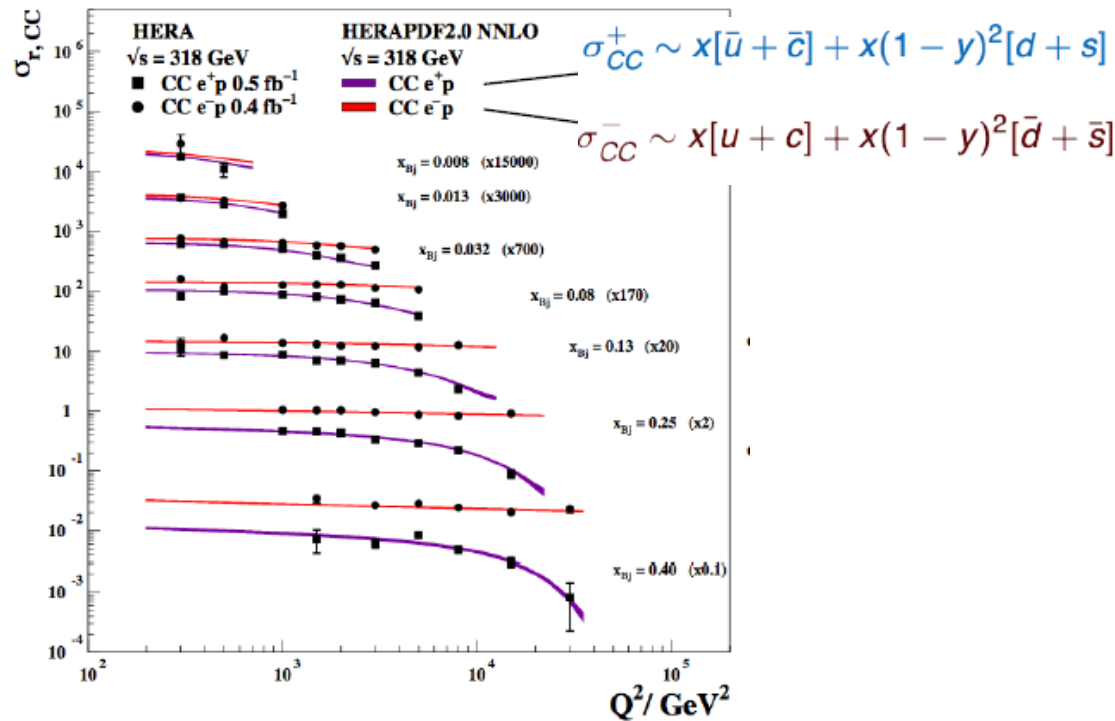
$Q = 100 \text{ GeV}$

CT14HERA2: test DGLAP factorization with combined HERA1+2 data!

H1 and ZEUS

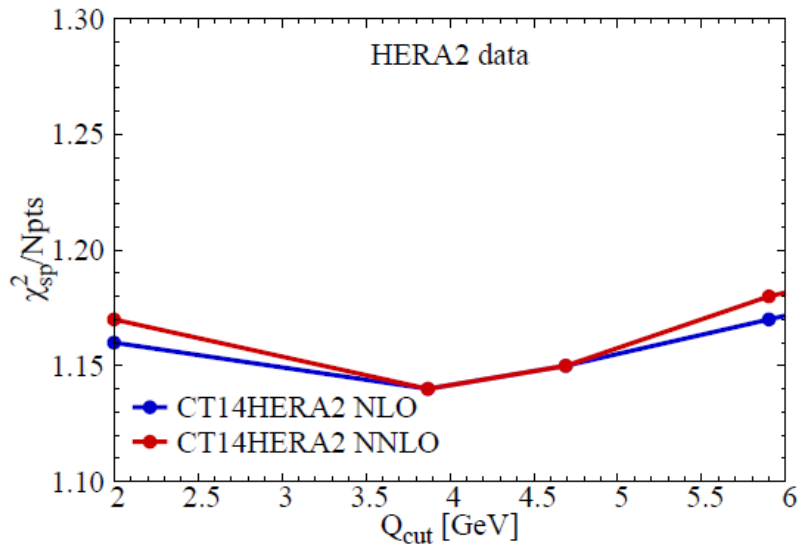
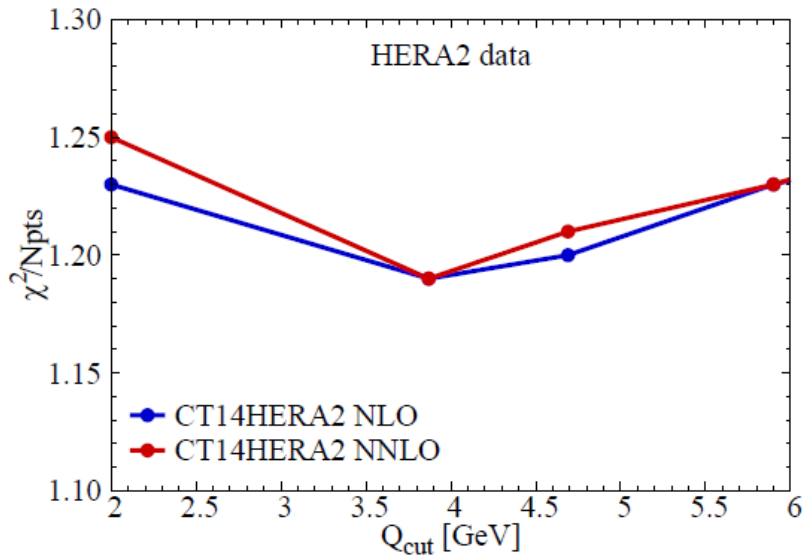


H1 and ZEUS



Combined H1 and ZEUS inc. cross sections in NC $e^\pm p$ and CC $e^\pm p$ DIS at $5 E_p$ with detailed correlation estimates (162 sources)

Strongly sensitive to u, g, c , less to d , and somewhat sensitive to $\bar{u}, \bar{d}, \bar{s}$ via CC cross sections



χ^2/N_{pts} with (top) and without (bottom) penalty for systematic shifts

The combined HERA1+2 data are included in HERA2.0, **CT14HERA2**, MMHT', and NNPDF3.1 analyses

$\chi^2/d.o.f. \sim 1.2$ for HERA1+2 tends to be elevated across all analyses, compared to < 1.1 for combined HERA1 data

⇒ This tension may arise from several sources

- Higher-twist corrections to $F_L(x, Q)$
A. Cooper-Sarkar, Harland-Lang et al.
 - Small- x /saturation *A. Luszczak*
 - Experimental systematics (?)
- Our preferred explanation**

The impact on global PDFs is mild, changes in PDFs do not exceed uncertainties

CT14 PDFs with HERA1+2 (=HERA2) combination

- Make the following changes with regards to CT14
 - replace HERA-1 ($N_{pt}=579$) by HERA-1+2 ($N_{pt} = 1120$)
 - remove NMC $F_2^p(x, Q)$ ($N=201$)
 - add 1 more parameter to strange quark PDF \Rightarrow slightly lower $s(x, Q)$

Separate the four HERA2 DIS processes;

($Q_{cut} = 2 \text{ GeV}$)

	N_{pts}	$\chi^2_{red.} / N_{pts}$
NC e^+p	880	1.11
CC e^+p	39	1.10
NC e^-p	159	1.45
CC e^-p	42	1.52
totals		
[reduced χ^2] / N	1120	1.17
χ^2 / N	1120	1.25
R^2 / N	1120	0.08

e^-p data is fitted poorly

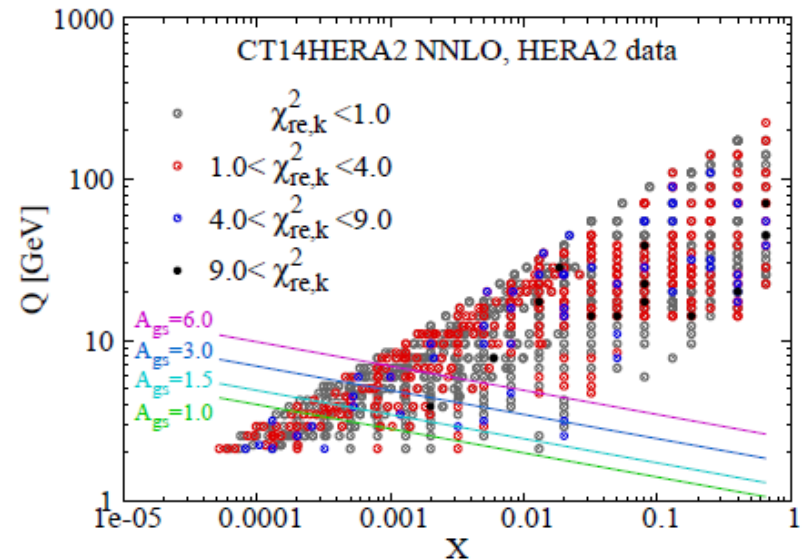
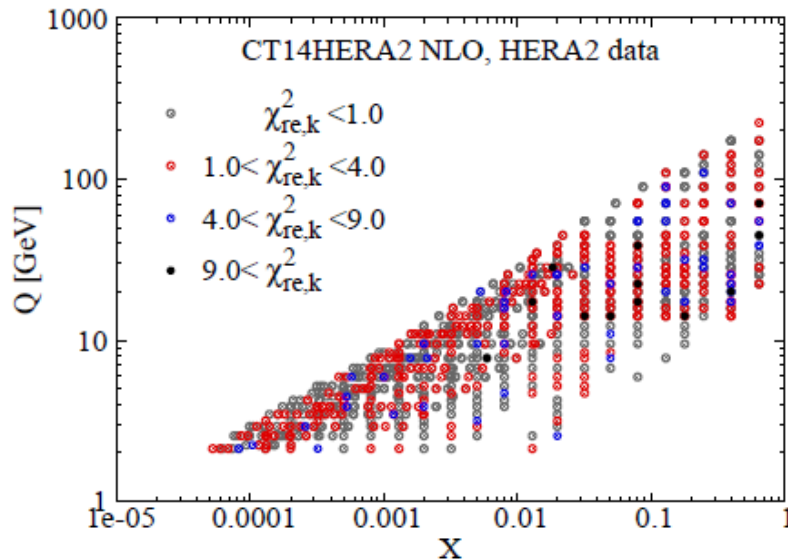
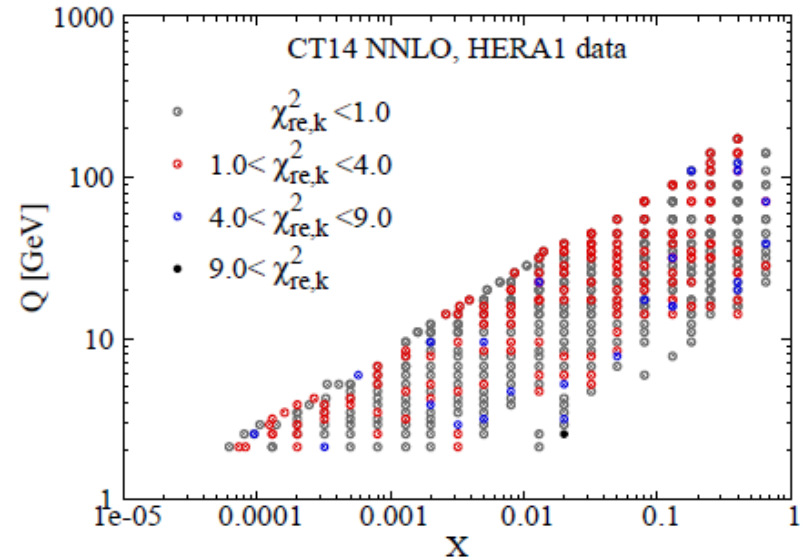
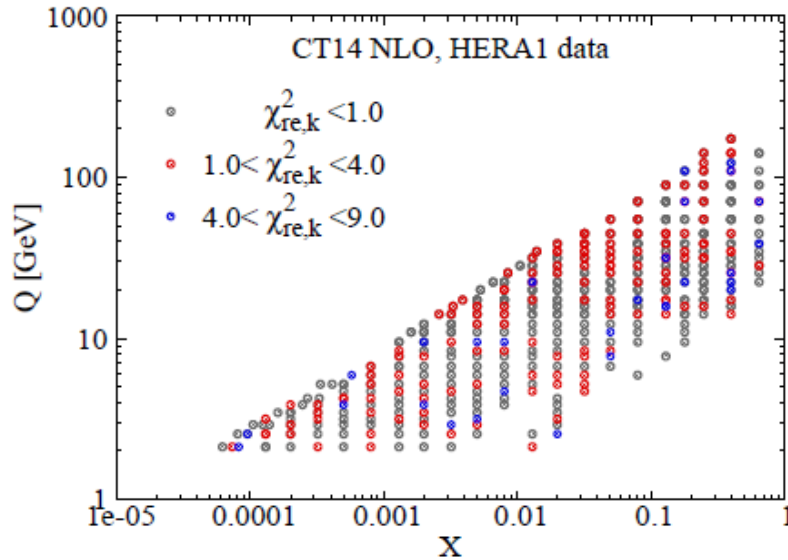
e^+p data is fitted fine

← reduced χ^2 values

← $\chi^2 = [\text{reduced } \chi^2] + R^2$

← The quadratic penalty for 162 systematic errors = 87.5

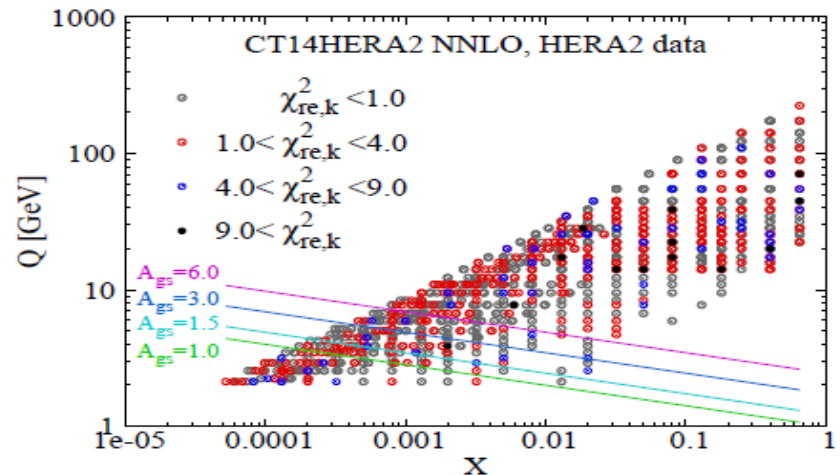
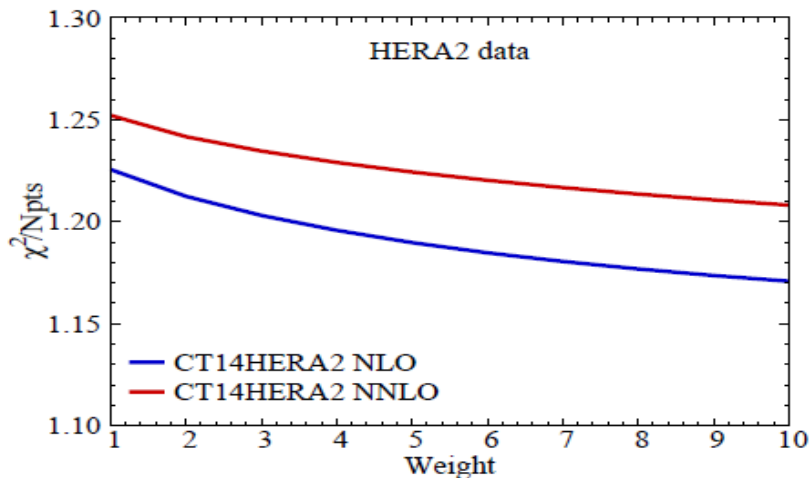
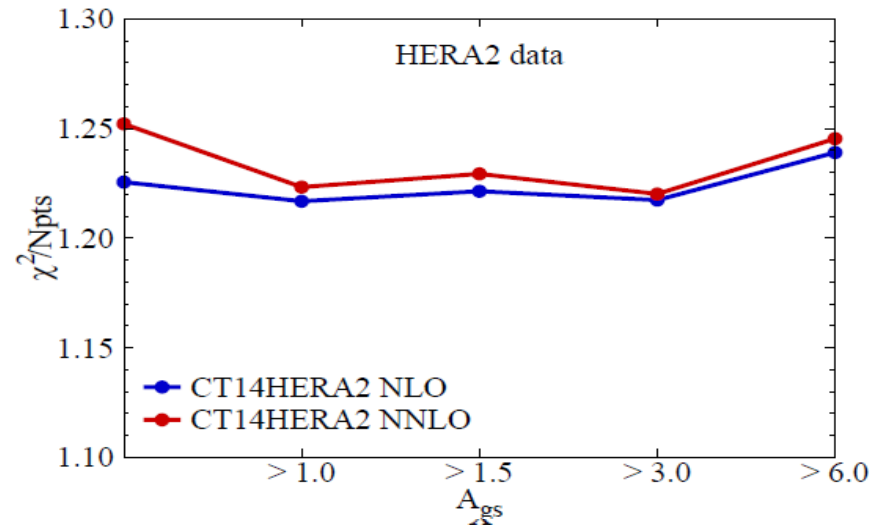
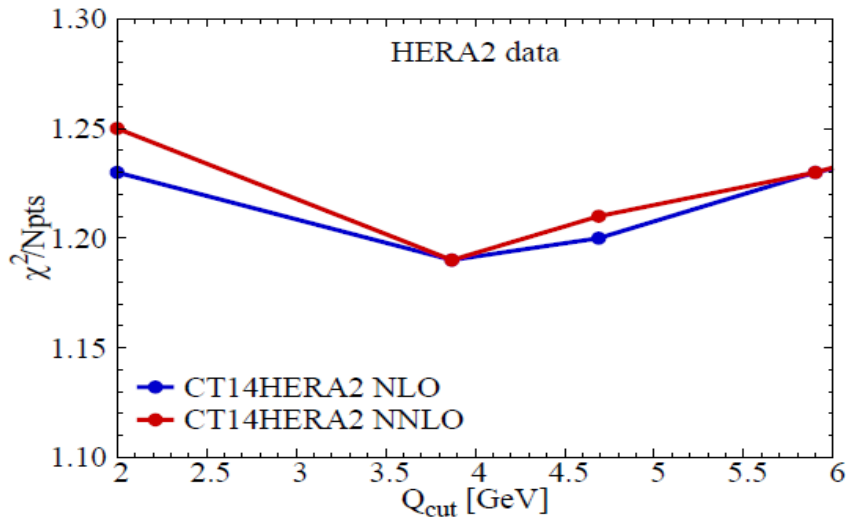
CT14 PDFs with HERA1+2 (=HERA2) data



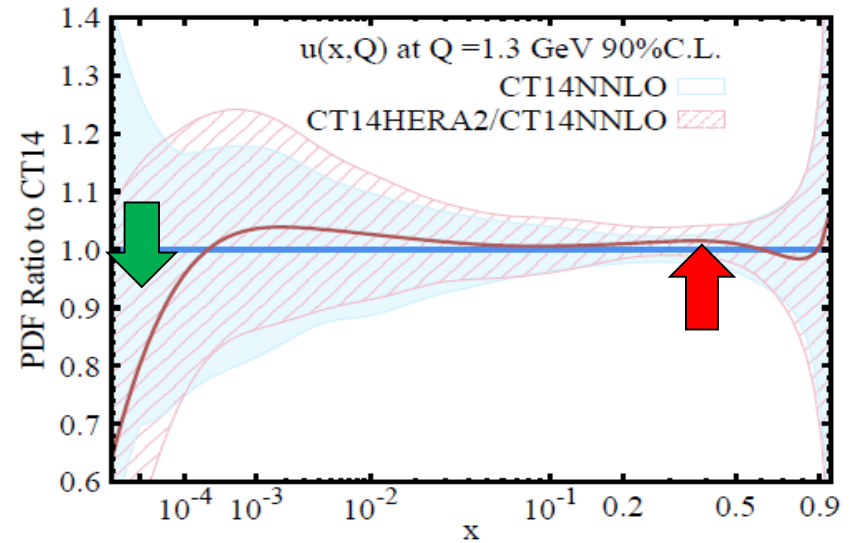
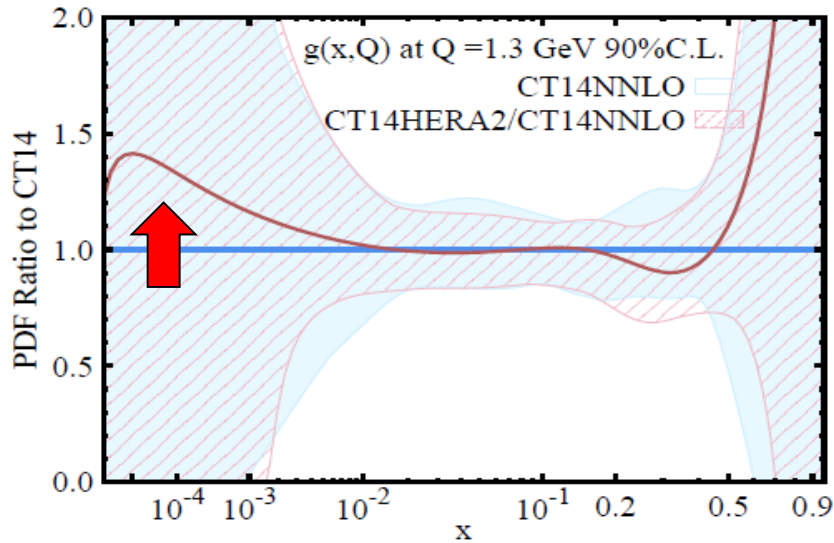
Points with excessive χ^2 are randomly scattered in the $\{x, Q\}$ plane

Stability of CT14 HERA2 fit

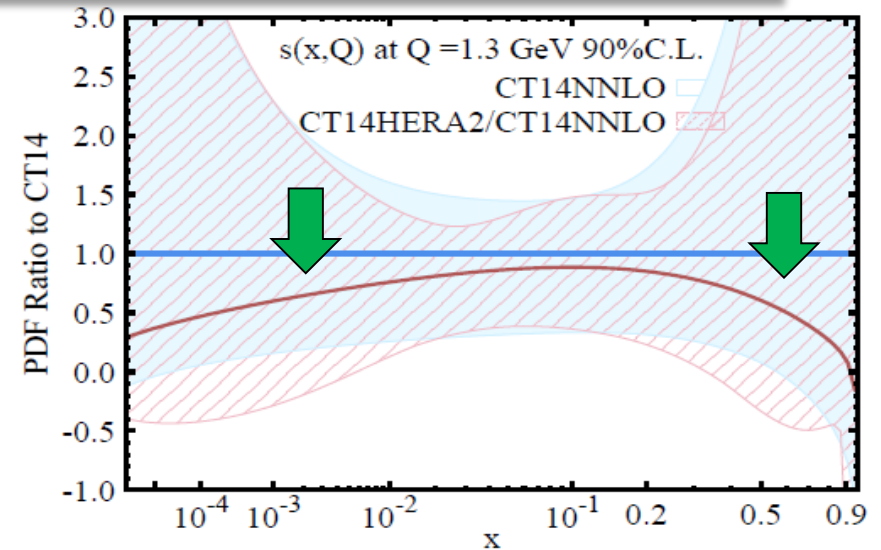
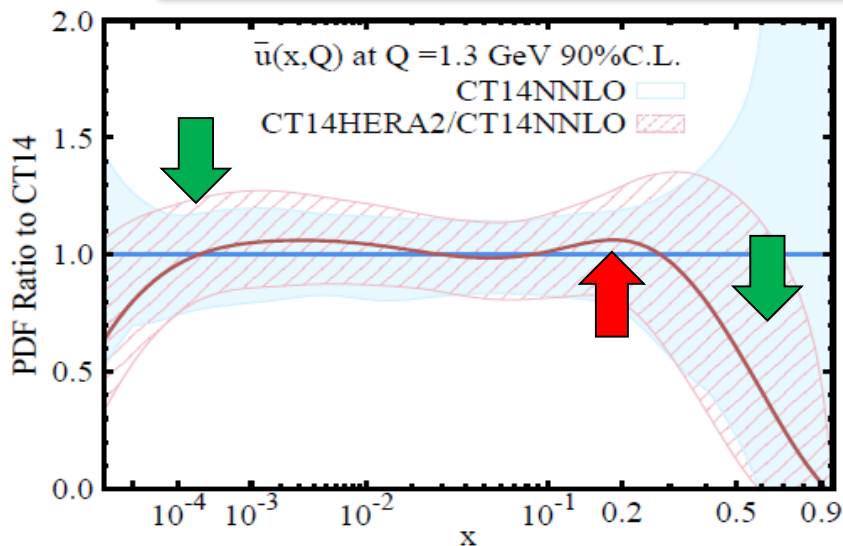
- The fit quality does not change much when we vary lower cuts on Q and $A_{gs} = x^{0.3} Q^2$, or increase statistical weight of the HERA2 data



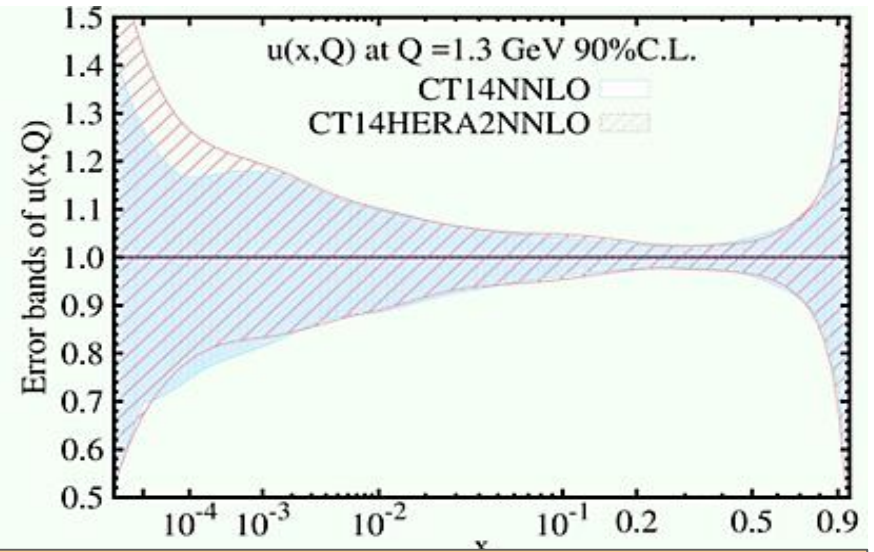
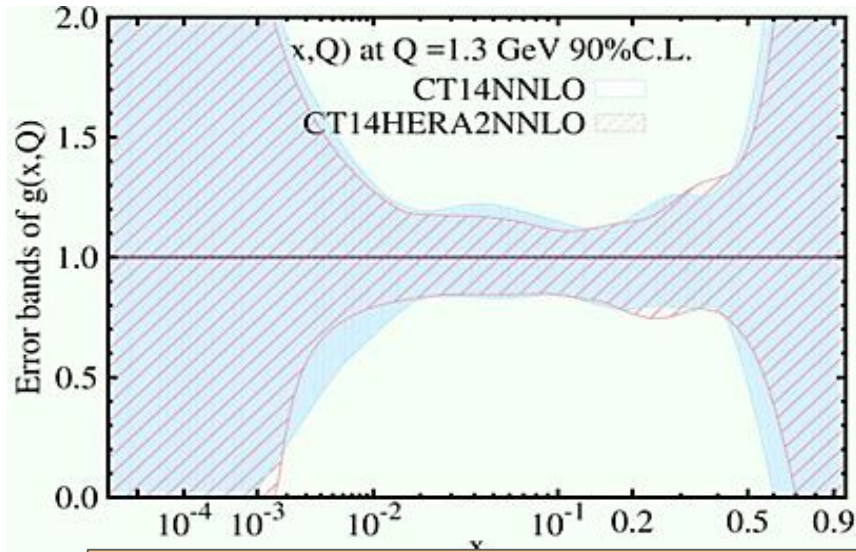
CT14HERA2 vs. CT14 PDFs: central sets



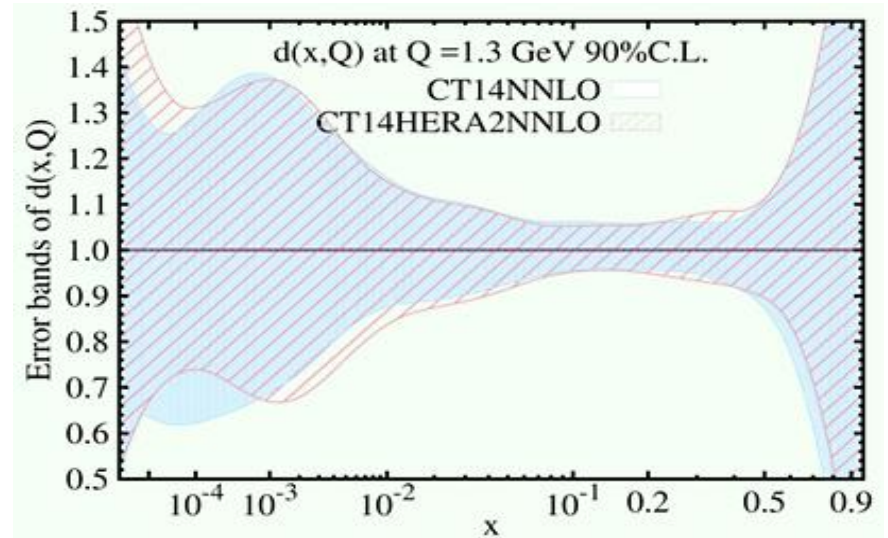
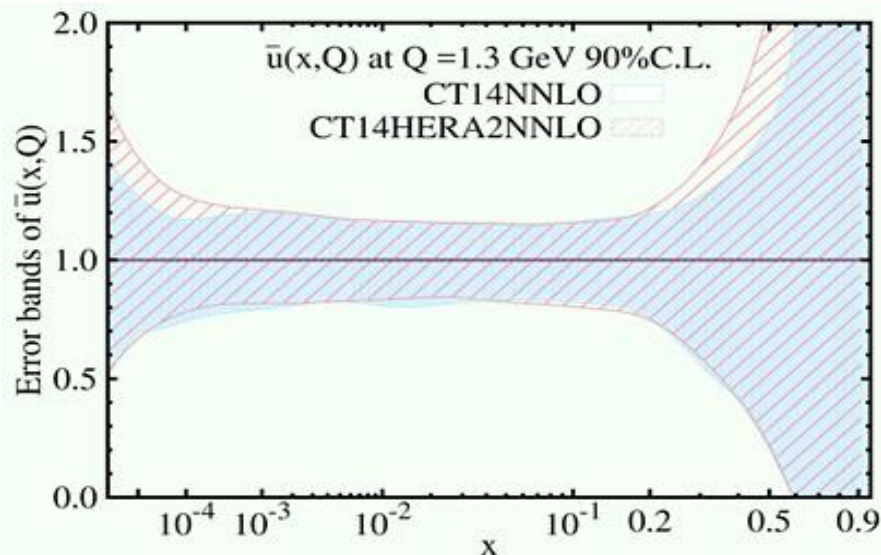
All changes are within CT14 uncertainties



CT14HERA2 vs. CT14 PDFs: % uncertainties



Uncertainty bands remain about the same



CT14 Monte-Carlo replica ensembles (MC1 and MC2) with asymmetric errors and positivity

arXiv:1607.06066

N_{rep} Monte-Carlo replicas are constructed from predictions $X_{\pm i}$ for Hessian eigenvector sets as

$$X^{(k)} = X(\{0\}) + \delta X^{(k)} - \Delta$$

$$\delta X^{(k)} \equiv \sum_{i=1}^D \frac{X_{+i} - X_{-i}}{2} R_i^{(k)} + \frac{1}{2} \sum_{i,j=1}^D (X_{+i} + X_{-i} - 2X_0) (R_i^{(k)})^2$$



Random real values $R_i^{(k)}$ are sampled from the standard normal distribution

CT14 MC1 replicas are constructed from $X = f_a(x, Q_0)$, can be negative

CT14 MC2 replicas are constructed from $X = \log [f_a/f_{a0}]$, where $f_{a0}(x, Q_0)$ is the central Hessian PDF; **each replica PDF is non-negative**

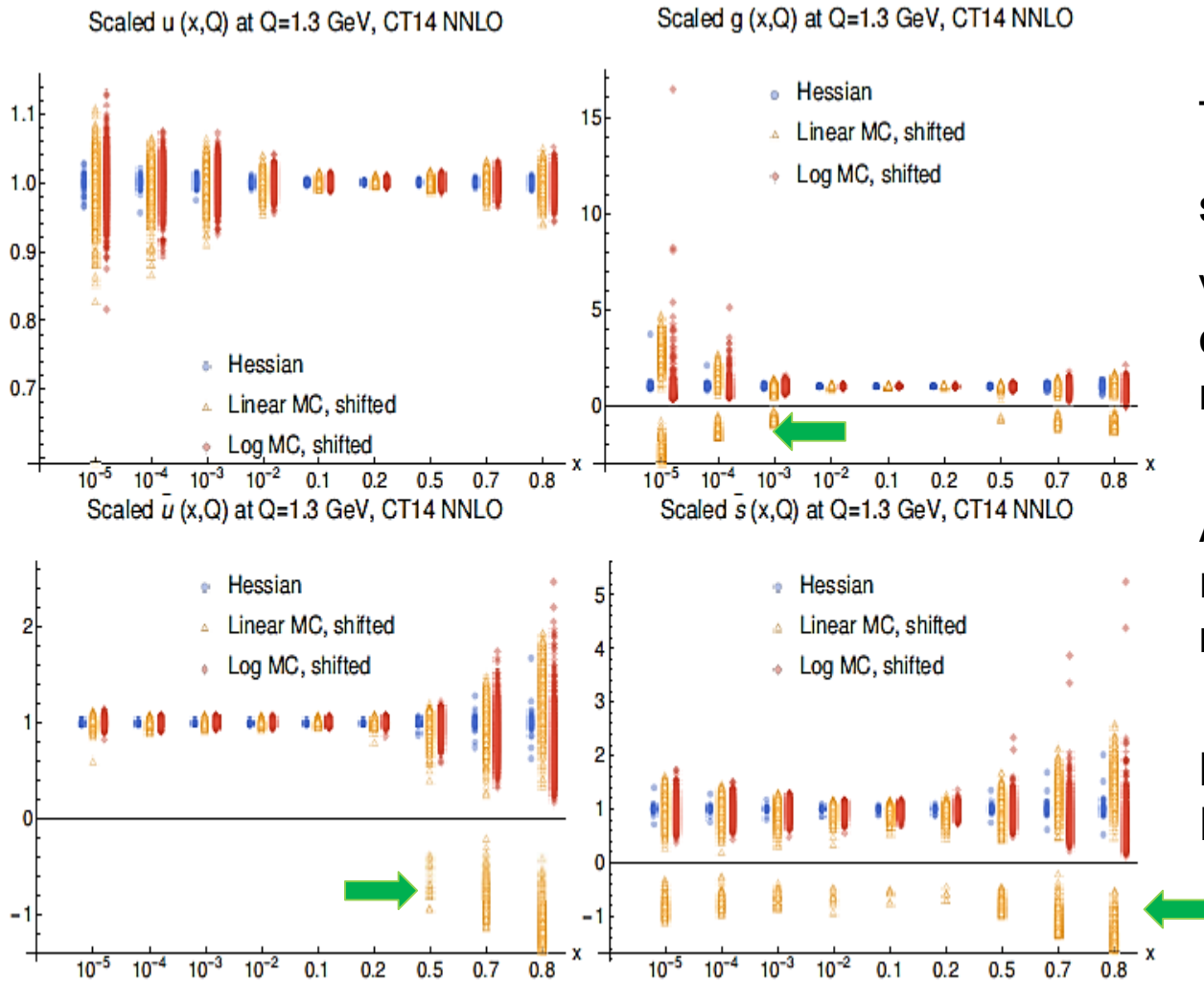
The uncertainties are given by **asymmetric** standard deviations,

$$\delta_{68}^{MC, >} X = \sqrt{\langle (X - \langle X \rangle)^2 \rangle_{X > \langle X \rangle}}$$

$$\delta_{68}^{MC, <} X = \sqrt{\langle (X - \langle X \rangle)^2 \rangle_{X < \langle X \rangle}}$$



f_a/f_{a0} values for individual replicas



The vertical axes have scale $\left| \frac{f}{f_{a0}} \right|^{0.2} \text{sign}(f)$ to visualize relative variations of \pm signs in an extended magnitude range

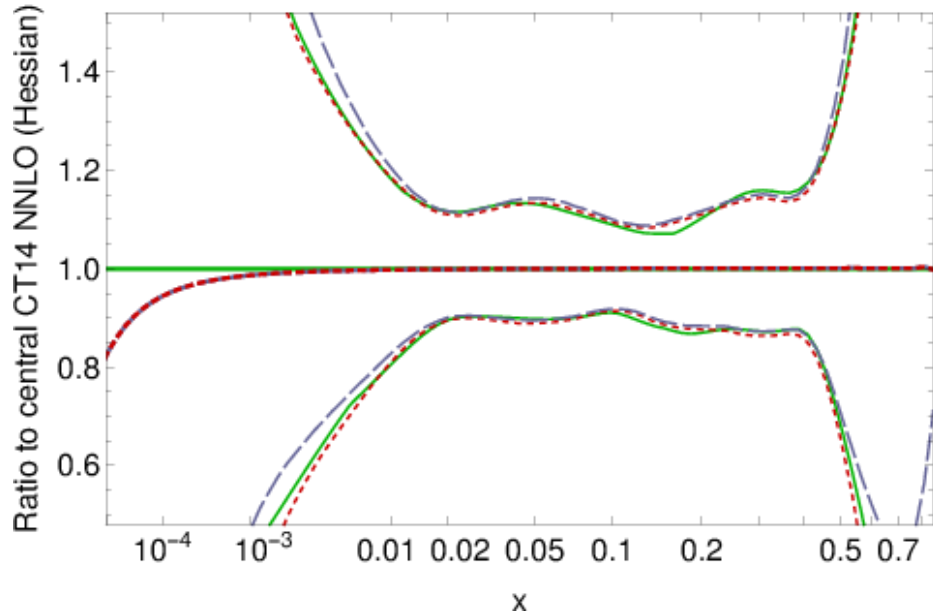
A fraction of 1000 MC1 replica PDFs can be negative (**green arrows**).

But, all Hessian and MC2 PDFs are positive

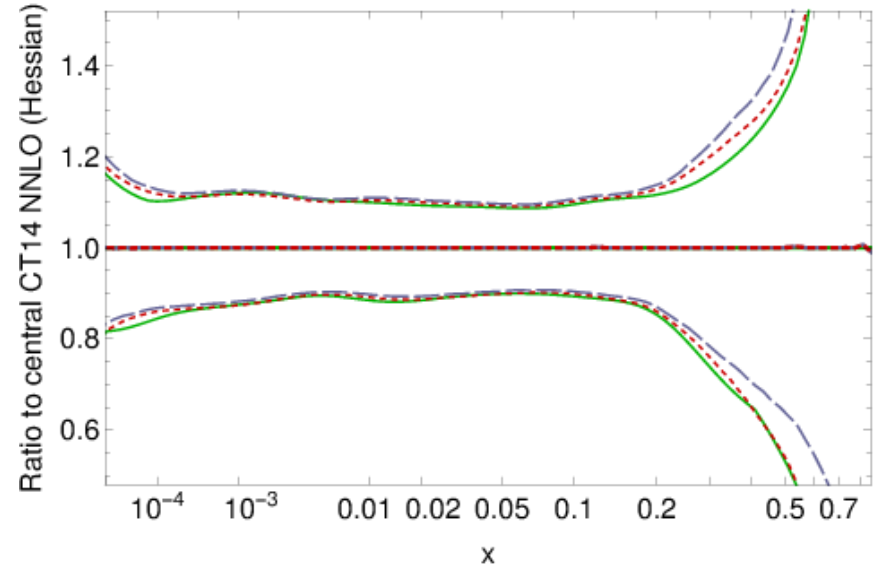
FIG. 2: Distributions of individual replicas for MC1 (linear MC, shifted) and MC2 (log MC, shifted) ensembles.

Asymmetric standard deviations for PDFs

$g(x, Q)$ at $Q=1.3$ GeV, CT14 NNLO, asym. std. dev.
Hessian, MC1, MC2: solid, short-dashed, long-dashed



$\bar{u}(x, Q)$ at $Q=1.3$ GeV, CT14 NNLO, asym. std. dev.
Hessian, MC1, MC2: solid, short-dashed, long-dashed



Excellent agreement between the Hessian, MC1, MC2 bands at intermediate x

More pronounced differences at small and large x ; there are ambiguities in reconstructing MC replicas from the Hessian PDFs when PDF uncertainties are large

Comparisons for other flavors at
<http://hep.pa.msu.edu/cteq/public/ct14/MC/>

PDFs with intrinsic charm (IC)

Several studies conclude that IC may carry no more than 1% of the proton's momentum

Constraints depend on data selection (e.g., on whether the EMC F_2^c data are included) and methodology (CTEQ vs. NNPDF)

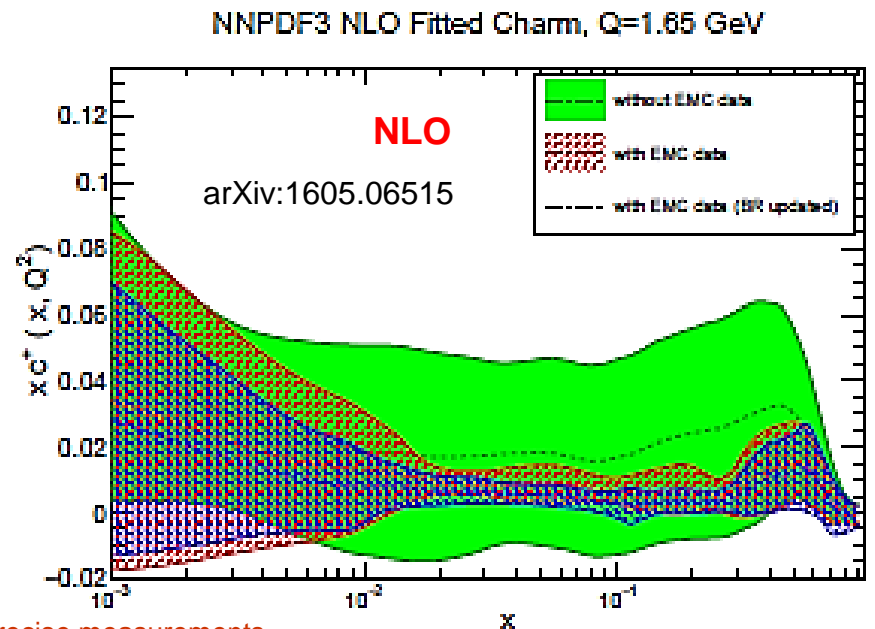
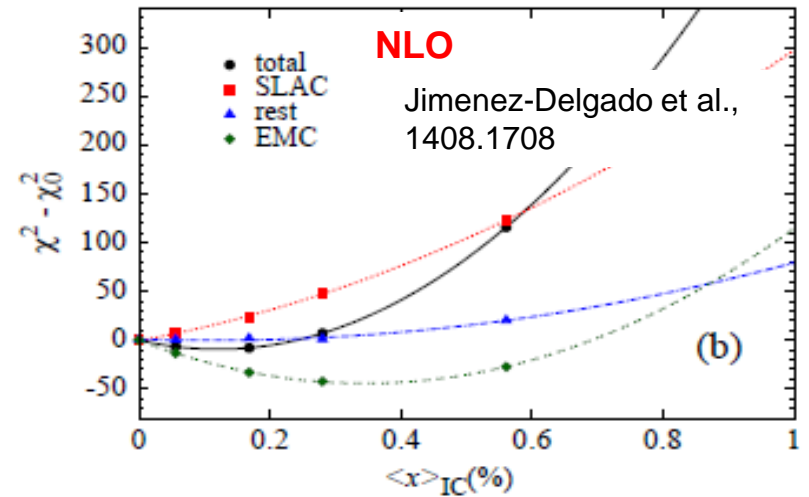
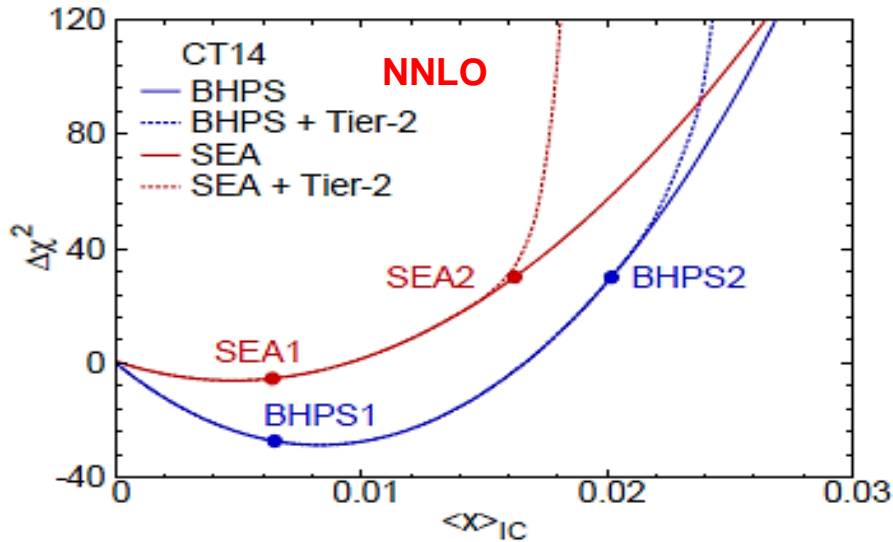
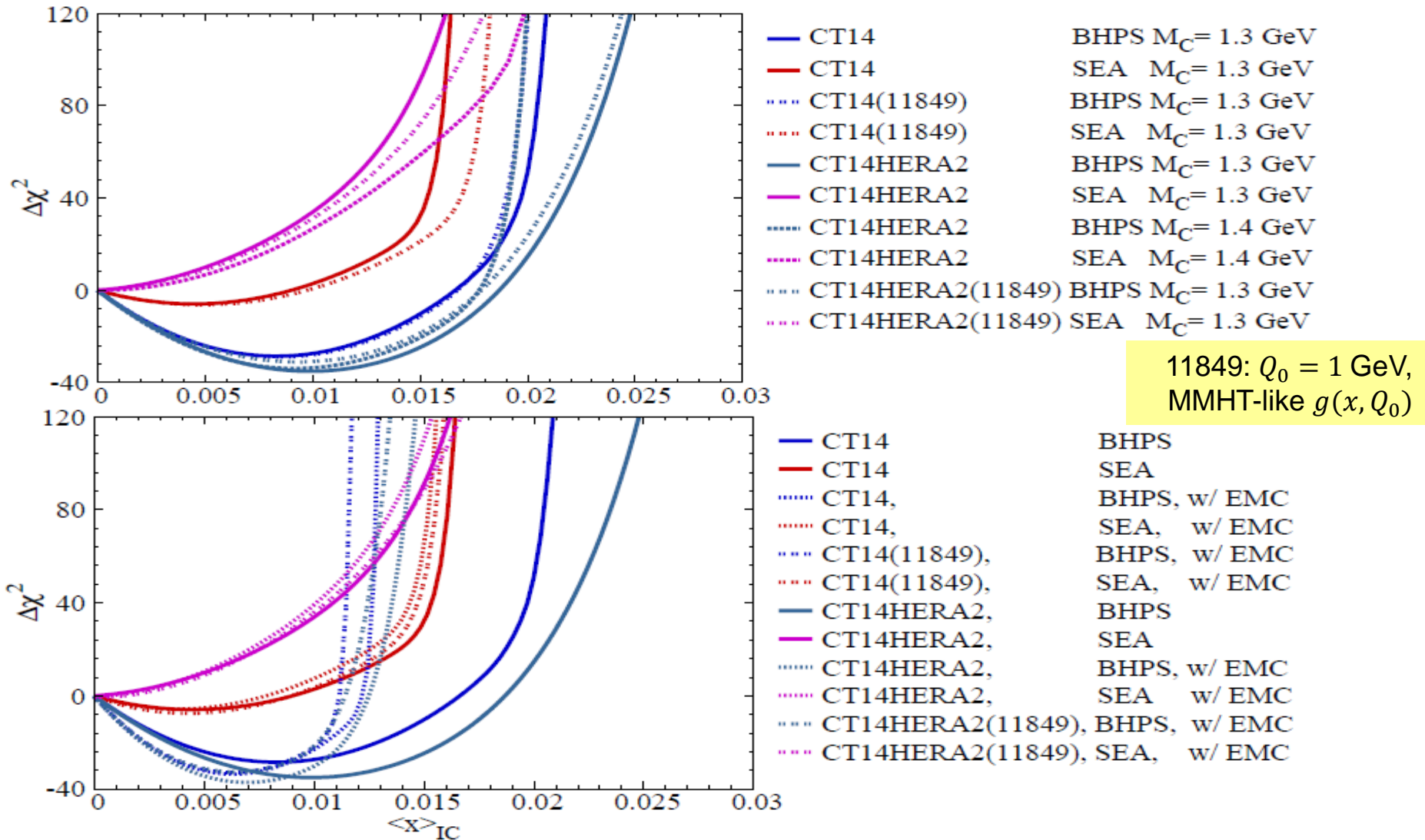


Figure 1: The $\Delta\chi^2$ versus the momentum fraction of charm $\langle x \rangle_{IC}$. PoS DIS2015 (2015) 166

In-depth study of CT14 IC fits (T.-J. Hou)



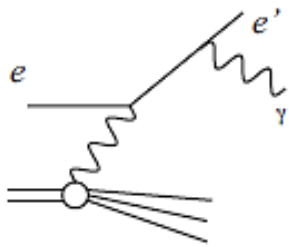
For the Brodsky-Hoyer-Peterson-Sakai (BHPS) parametrization,

a **marginally** better χ^2 for IC with $\langle x \rangle_{IC} \approx 1\%$

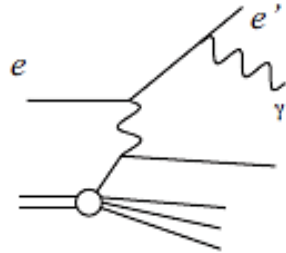
For SEA parametrization, IC with $\langle x \rangle_{IC} \approx 1.5\%$ is allowed within uncertainty

CT14 QED PDFs

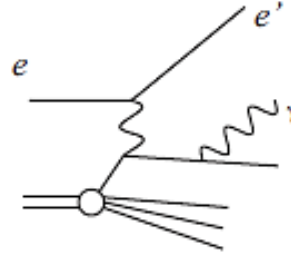
C. Schmidt, J. Pumplin, D. Stump, C.-P. Yuan, arXiv:1509.02905



$$|M|_{\gamma\gamma}^2$$



$$|M|_{LL}^2$$



$$|M|_{QQ}^2 + \text{interference}$$

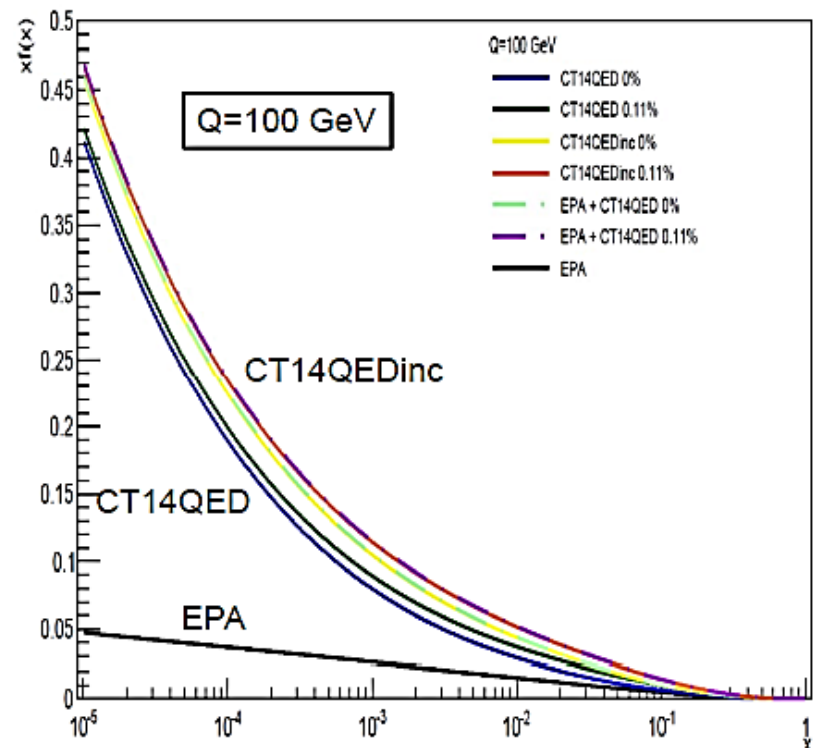
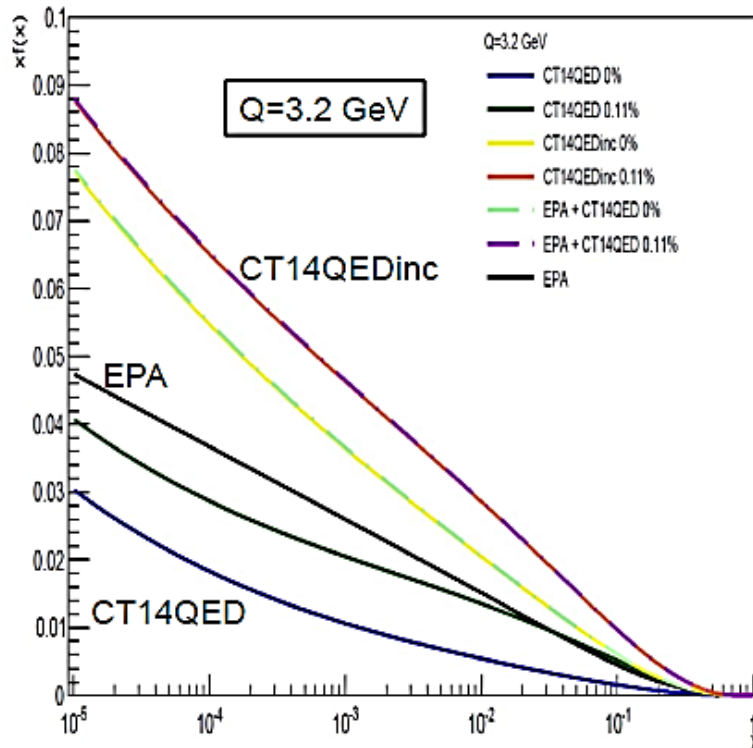
ZEUS $ep \rightarrow e\gamma X$ data
($N_{pt} = 8$) included to
constrain $f_\gamma(x, Q)$

Still in exploratory stage – limited experimental constraints, further theory developments needed (full NNLO QCD+(N)LO EM DGLAP evolution code, consistent EW corrections to all fitted cross sections)

$u^p(x, Q) \neq d^n(x, Q)$ -- need more data to resolve difference

Photon momentum fractions $> 0.14\%$ at Q_0 are disfavored, for the given isolation models

CT14QED and CT14QEDinc PDFs

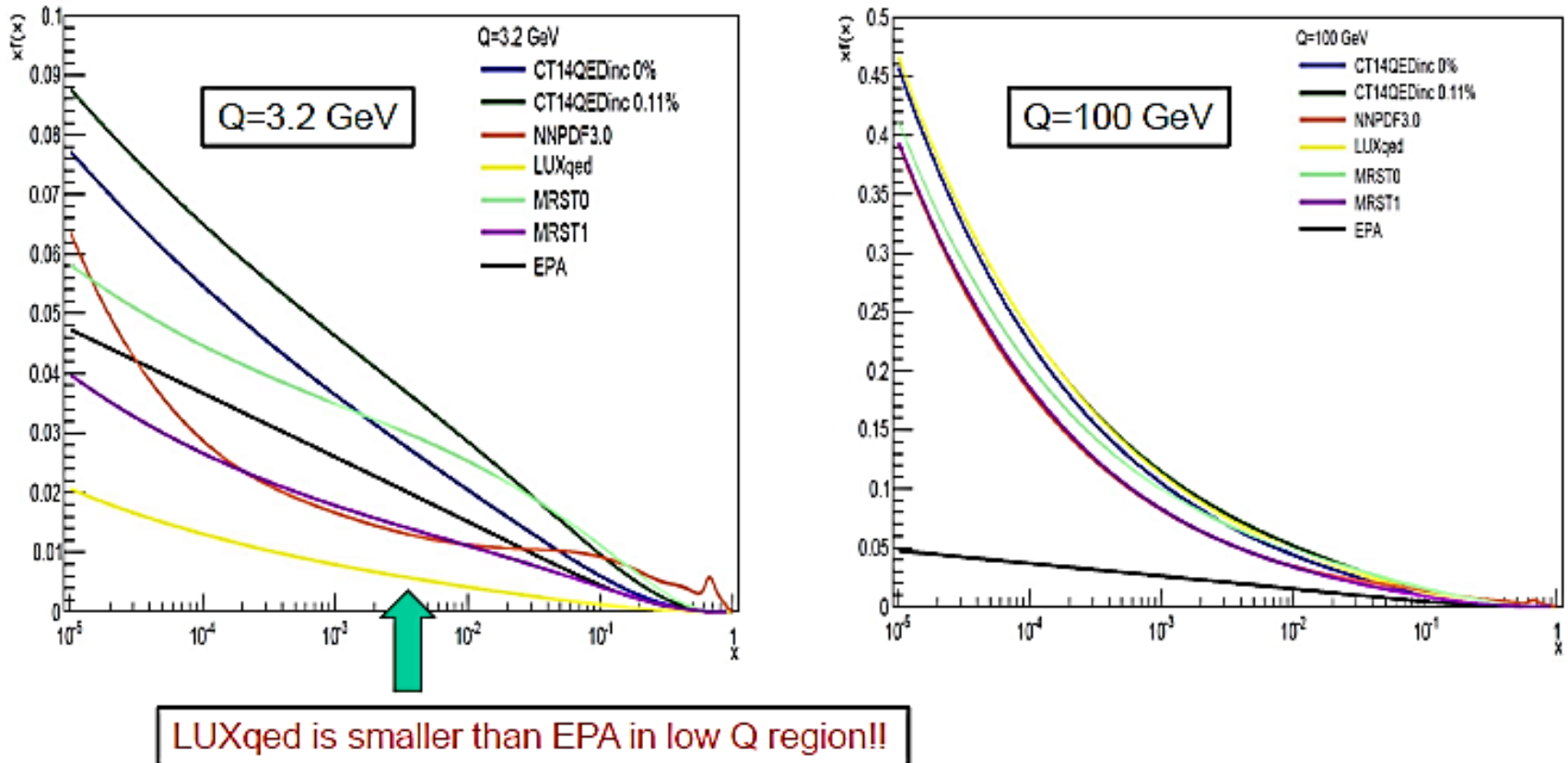


Boundary condition at $Q_0 = 1.3$ GeV

- **CT14QED**: only inelastic radiation $ep \rightarrow e\gamma X$
- **CT14QEDinc** also includes photon radiation from $ep \rightarrow e\gamma p$ in the equivalent photon approximation (EPA)

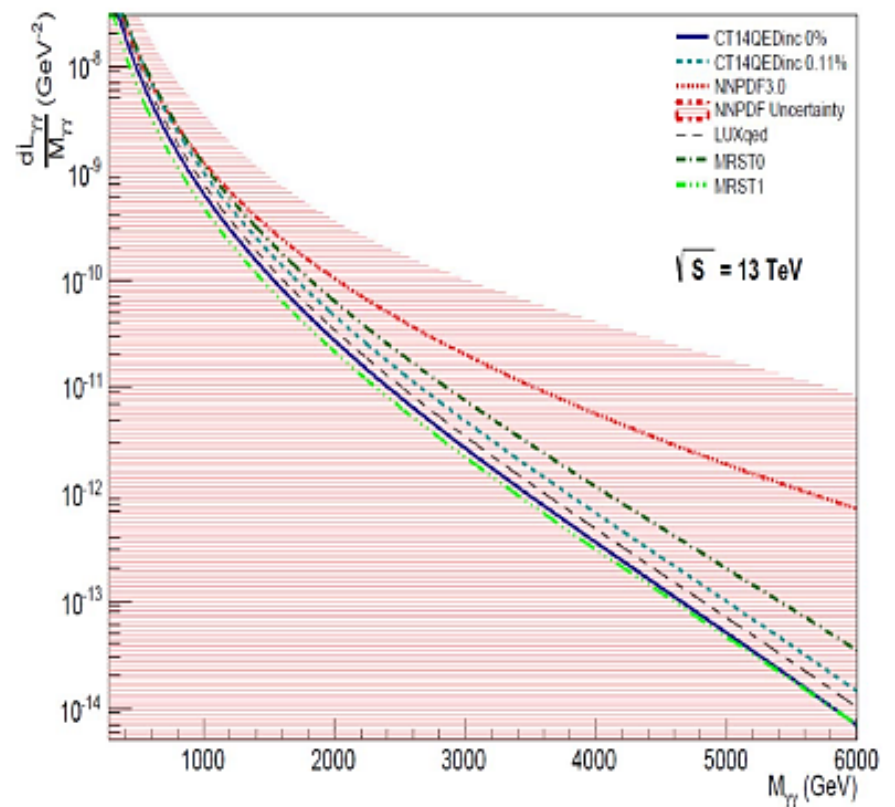
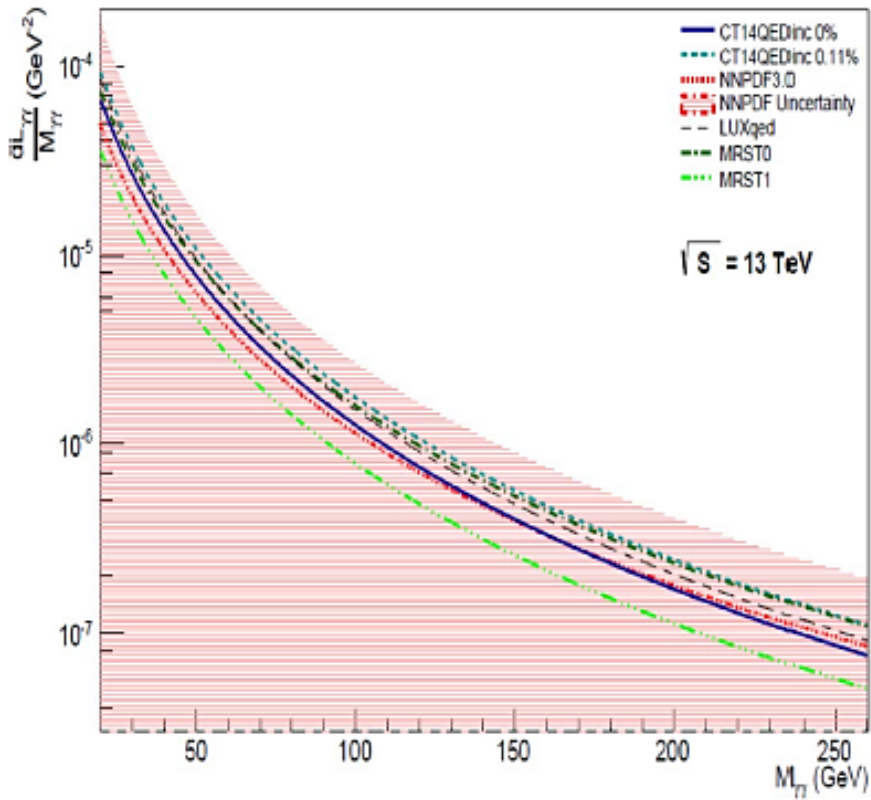
Photon PDFs are evolved to higher Q at LO in α_{EM} and NLO in α_S

Comparison of QCD+QED PDFs



Uncertainty bands cover most central predictions

Parton-parton luminosity

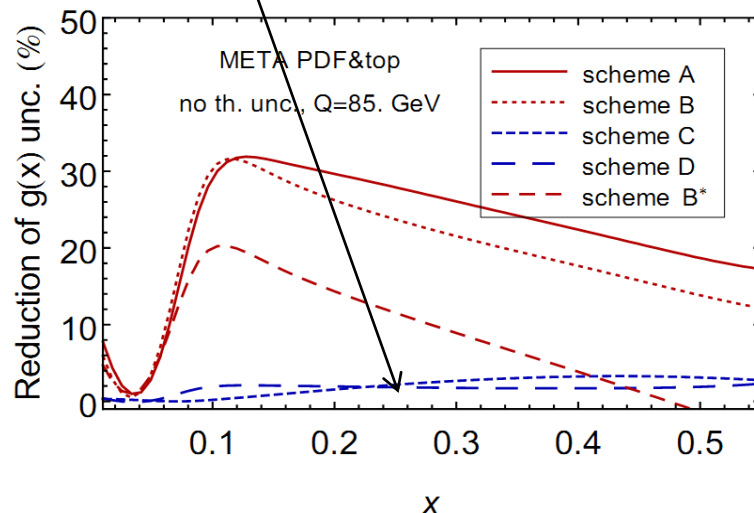


Ongoing work: inclusion of new LHC data

- W/Z , $t\bar{t}$ differential
 - applgrid at NLO with NNLO/NLO K-factors
 - Understand tensions between ATLAS and CMS
- Inclusive jets
 - will continue to use NLO and fastNLO/applgrid to include 8 and 13 TeV ATLAS/CMS jet data sets
 - NNLO corrections were shown to be small when correct scale is used; no need for rapidity cuts
 - will adapt to NNLO format when available
- Photon/ W/Z +charm
 - some theoretical work ongoing before inclusion in global PDF fit
 - framework for charm will continue to be perturbative charm, without an intrinsic component

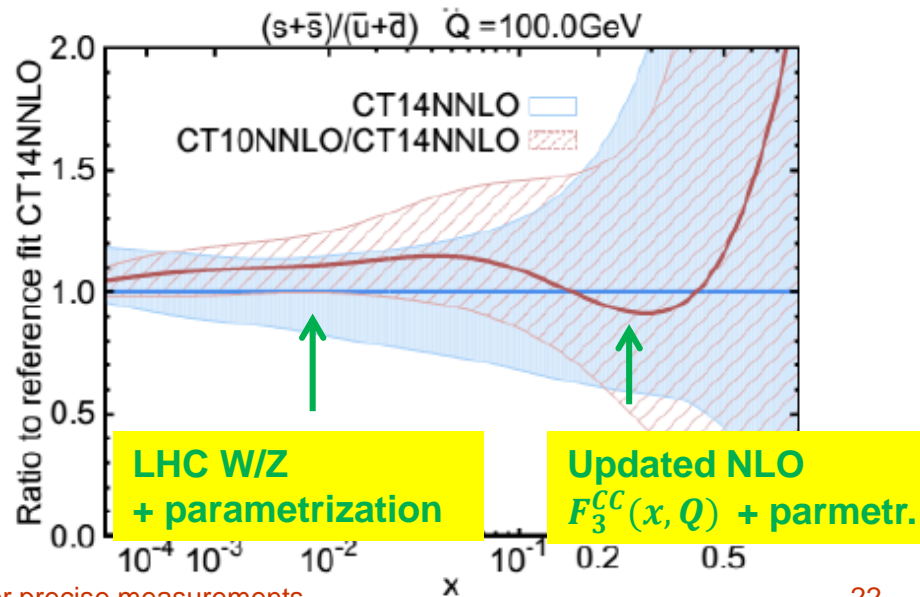
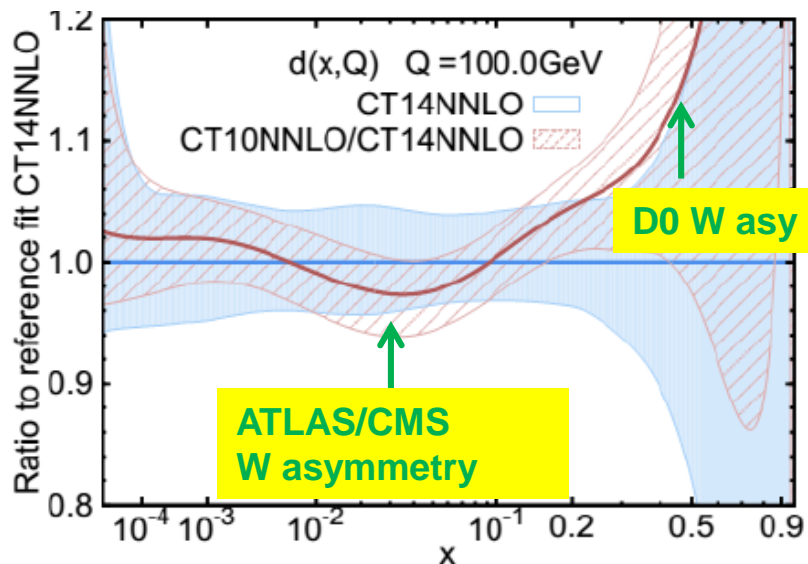
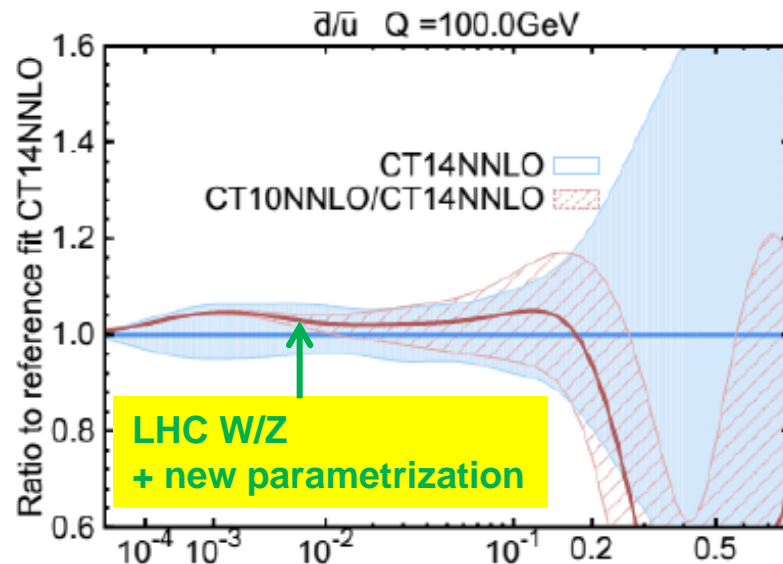
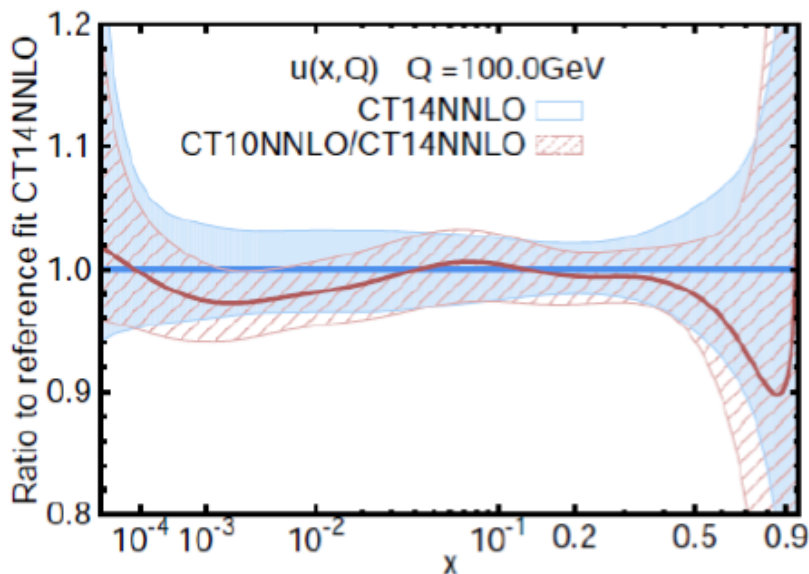
- In general, we are working on improving the speeds of NLO and NNLO fits
- PDF re-weighting is being explored, but has to take into account tolerance issues
- For example, for global PDF fits like MMHT or CT, reduction in χ^2 for $t\bar{t}$ total cross section (1303.7215) less significant than suggested by re-weighting

Jun Gao



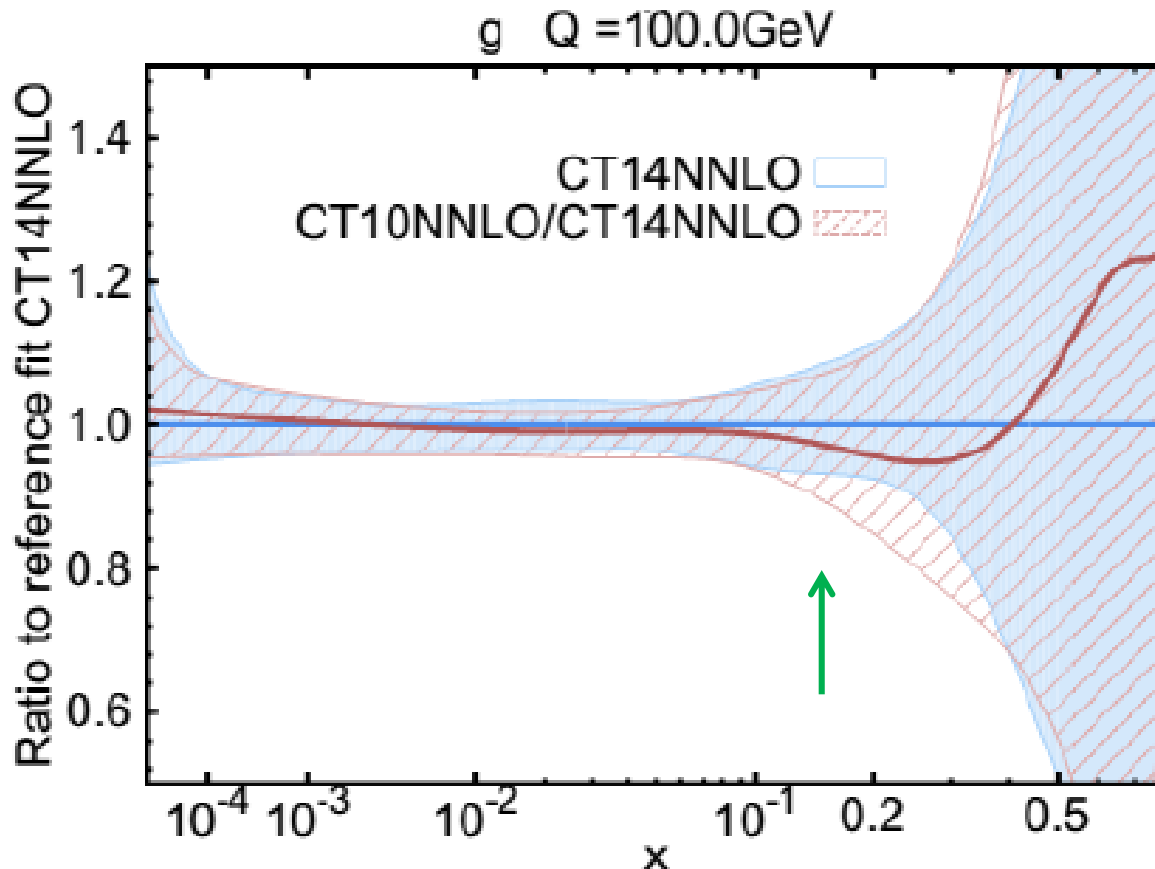
Backup slides

Compare CT14 and CT10 quark PDFs



CT14 vs. CT10: the gluon PDF

$g(x, Q)$ is slightly higher in CT14 at $x \sim 0.05$ because of several effects.



CT14 Higgs cross sections increase compared to CT10 by about 1-2%

A “significant” change by LHC standards, given that the N3LO theory uncertainties are $\sim 3\%$

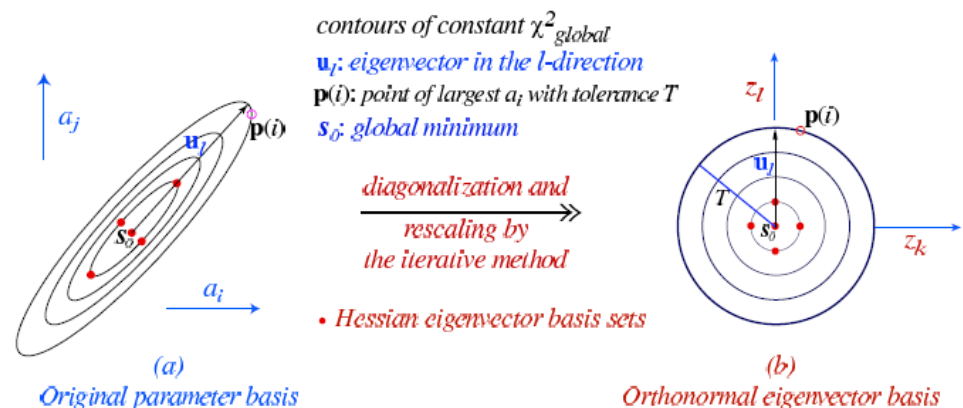
The net NNLO PDF uncertainty on σ_H is $\approx 3\%$

Generation of MC replicas from CT14 Hessian eigenvector sets

MC replicas for PDFs $f_a(x, Q) \equiv f \dots$

- are constructed from the best-fit (central) PDF values f_0 and 68% c.l. extreme displacements $f_{\pm i}$ along eigenvector directions $\vec{u}_i, i = 1, \dots, 28$ in parameter space near χ^2 minimum
- retain exact information about boundaries of 68% or 90% probability regions; approximate probability everywhere using Gaussian approximation
- approximate asymmetric Hessian errors using modified standard deviations

2-dim (i,j) rendition of d-dim (~20) PDF parameter space



What is intrinsic charm, according to QCD theory?

The ACOT family of schemes used by CTEQ fits are uniquely suited for establishing physical properties of the “intrinsic charm”.

- The FFN scheme and ACOT schemes are proved by the QCD factorization theorem with explicit power counting of scattering contributions at $p^+ \rightarrow \infty$
- Factorization for another GM-VFN scheme (FONLL, TR', ...) can be demonstrated, e.g., by reducing to a counterpart ACOT scheme order by order in α_s

At $Q^2 \approx m_c^2$, the ACOT $N_f = 4$ scheme reduces to the $N_f = 3$ scheme, order by order in α_s

In the $N_f = 3$ scheme, (Collins 1998) proved that, at $Q^2 \approx m_c^2$,

$$F_2(x, Q^2) = \underbrace{\sum_{a=u,d,s,g} \int_x^1 \frac{dz}{z} C_a \left(\frac{x}{z}, \frac{m_c^2}{Q^2}, \frac{\mu^2}{Q^2} \right) f_a(z, \mu^2)}_{\text{leading power (l.p.)}} + O(\Lambda^2)$$

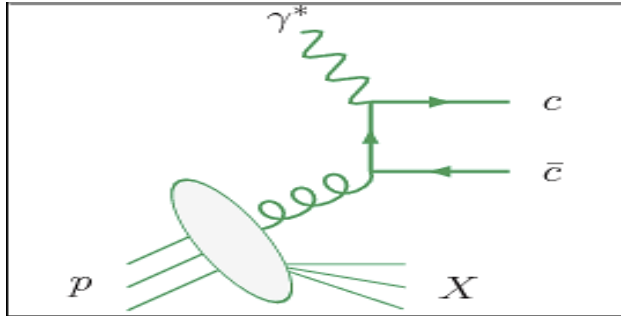
- The l.p. term contains charm propagators only in the coefficient functions, sums only over light-flavor PDFs

⇒ In either the $N_f = 3$ scheme or ACOT scheme at $Q^2 \approx m_c^2$ and $O(\alpha_s^n)$, the phenomenological IC term is composed of $O(\alpha_s^{n+1})$ l.p. terms and $O(\frac{\Lambda^2}{m_c^2})$

terms

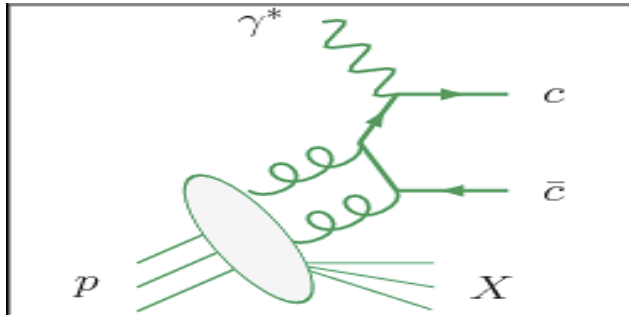
Charm scattering contributions at $Q^2 \approx m_c^2$, sample diagrams

Leading-power charm



- Single-parton scattering
- Of order $\left(\frac{m_c^2}{Q^2}\right)^k$
- All-order \overline{MS} formalism to factorize into hard cross sections and light-parton PDFs
- When matched onto the $N_f = 4$ scheme, gives rise to **process-independent** charm PDFs

Fitted (intrinsic) charm



- Multi-parton scattering
- Of order $(\Lambda^2/m_c^2)^k$
- A power-suppressed correction to the factorized QCD cross section
- Currently not covered by the \overline{MS} factorization theorem; **“IC PDF” can be process-dependent**

Consequences for interpretation of IC PDFs

The phenomenological IC PDF is a model for $O(\alpha_s^{n+1})$ l.p. and $O\left(\frac{\Lambda^2}{m_c^2}\right)$ scattering terms. The standard formalism does not tell us how to factorize the IC contributions into hard perturbative and universal nonperturbative parts. Nevertheless, the CT14 NNLO IC PDFs can be used for first estimates of sensitivity of LHC cross sections to charm scattering contributions beyond l.p. QCD. **[If used with caution!]**